Nat. Hazards Earth Syst. Sci. Discuss., doi:10.5194/nhess-2017-123, 2017
Manuscript under review for journal Nat. Hazards Earth Syst. Sci.
Discussion started: 19 April 2017

Width of surface rupture zone for thrust earthquakes. Implications for earthquake fault zoning.

Paolo Boncio[1], Francesca Liberi[1], Martina Caldarella[1], Fiia C.Nurminen[2]
[1]CRUST-DiSPUTer,"G. D'Annunzio" University of Chieti-Pescara, Chieti, I-66100, Italy
[2]Oulu Mining School, University of Oulu, Oulu, FI-90014, Finland
Correspondence to: Paolo Boncio (paolo.boncio@unich.it)

Abstract. The characteristics of the zones of coseismic surface faulting along thrust faults are analysed in order to define the criteria for zoning the Surface Fault Rupture Hazard (SFRH) along thrust faults. Normal and strike-slip faults have been deeply studied in the past concerning SFRH, while thrust faults have not been studied with comparable attention.

Surface faulting data were collected from 10 well-studied historic thrust earthquakes occurred globally (5.4 ≤ M ≤ 7.9). Several different types of coseismic fault scarps characterise the analysed earthquakes, depending on the topography, fault geometry and near-surface materials (simple and hanging wall collapse scarps; pressure ridges; fold scarps and thrust or pressure ridges with bending-moment or flexural-slip secondary faults due to large-scale folding). For all the earthquakes, the distance of secondary ruptures from the main fault (r) and the width of the rupture zone (WRZ) were collected directly from the literature or measured systematically in GIS-georeferenced published maps.

Overall, surface ruptures can occur up to large distances from the main fault (~750 m on the footwall and ~1,600 m on the hanging wall). Most of them occur on the hanging wall, preferentially in the vicinity of the main fault trace (< 50 m). The widest WRZ are recorded where bending-moment (B-M) or flexural-slip (F-S) secondary faults, associated to large-scale folds (hundreds of meters to kilometres in wavelength), are present.

The distribution of surface ruptures is fitted with probability density functions, in order to define a criterion to remove outliers (e.g. 90% probability of the cumulative distribution function) and define the zone where the likelihood of having surface ruptures is the highest. This might help in sizing the zones of SFRH during seismic microzonation (SM) mapping.

In order to shape zones of SFRH, a very detailed earthquake geologic study of the fault is necessary (the highest level of SM, i.e., Level 3 SM according to Italian guidelines). In the absence of such a very detailed study (basic SM, i.e., Level 1 SM of Italian guidelines) a width of ~465 m (90% probability) seems to be adequate. For more

Nat. Hazards Earth Syst. Sci. Discuss., doi:10.5194/nhess-2017-123, 2017
Manuscript under review for journal Nat. Hazards Earth Syst. Sci.
Discussion started: 19 April 2017

Natural Hazards and Earth System Sciences
Open Access
Discussions

detailed level SM, where the fault is carefully mapped, one must consider that the highest SFRH is concentrated in a narrow zone, only 50-70 in width , that should be considered as a fault avoidance zone (40-50% of the total ruptures are expected to occur within this zone).
A broad positive relation between the displacement on the main fault and the total width of the rupture zone is found only close to the main fault (total WRZ $\leq$ 60 m). The total WRZ appears to increase with displacement, from a minimum of nearly 20-30 m for decimetric vertical displacement up to 50-60 m for vertical displacement close to 2 m.
The fault zones should be asymmetric compared to the trace of the main fault. The average footwall to hanging wall ratio (FW: HW) is close to 1:2.
These criteria are applicable to "simple thrust faults", without B-M or F-S secondary faults on large-scale folds. Zones potentially susceptible to B-M or F-S secondary faults can be inferred by detailed knowledge of the structural setting of the area (geometry, wavelength and lithology of the thrust-related large-scale folds) and by geomorphic evidence of past secondary faulting.

Key words

Fault rupture hazard, thrust earthquakes, earthquake fault zoning.

1 Introduction

Coseismic surface ruptures during large earthquakes might produce damage to buildings and facilities located on or close to the trace of the active seismogenic fault. This is known as Surface Fault Rupture Hazard (SFRH), a localized hazard that could be avoided if a detailed knowledge of the fault characteristics is achieved. The mitigation of SFRH can be faced by strategies of fault zoning and avoidance or, alternatively, by (or together with) probabilistic estimates of fault displacement hazard (e.g. Petersen et al., 2011). Both strategies need to employ, as accurately as possible, the location of the active fault trace, the expected displacement on the main fault, the deformation close to the main fault, and the distribution of secondary faulting away from it. While the general fault geometry and the expected displacement can be obtained through a detailed geological study and the application of empirical relationships (e.g. Wells and Coppersmith, 1994), the occurrence of secondary faulting close to and away from the main fault is particularly difficult to predict, and only direct observations from well-documented case studies may provide insights on how secondary faulting is expected to occur (e.g. shape and size of rupture zones, attenuation relationships for secondary faulting).

A reference example of fault zoning strategy for mitigating SFRH is the Alquist-Priolo Earthquake Fault Zoning Act (A-P Act), adopted by the state of California (USA) in 1972 (e.g. Bryant and Hart, 2007). The A-P Act defines regulatory zones around active faults (Earthquake Fault Zones, EFZ), within which detailed geologic investigations are required prior to build structures for human occupancy. The boundaries of the EFZ are placed 150-200 m away from the trace of major active faults, or 60 to 90 m away from well-defined minor faults, with exceptions where faults are complex or not vertical. Moreover, the A-P Act defines a minimum distance of 50 feet (15 m) from the well-defined fault trace within which critical facilities and structures designed for human occupancy cannot be built (fault setback), unless proven otherwise. Similarly to the setback of the A-P Act, the New Zealand guidelines for development of land on or close to active faults (Kerr et al., 2003) define a fault avoidance zone to ensure life safety. The guidelines recommend a minimum buffer of 20 m either sides of the known fault trace (or the likely rupture zone), unless detailed fault studies prove that the deformed zone is less than that.

Recently, in Italy the Department for Civil Protection published guidelines for land management in areas affected by active and capable faults. For the purpose of the guidelines, an active and capable fault is defined as a fault with demonstrated evidence of surface faulting during the last 40,000 years (Technical Commission for Seismic Microzonation, 2015; SM Working Group, 2015). The guidelines are a tool for zoning active and capable faults during seismic microzonation (SM). They also contain a number of recommendations to assist land managers and planners. The fault zones vary at different Levels of SM. In the basic SM (Level 1 SM according to SM Working Group, 2015), the active fault is zone with a wide Warning Zone that is conceptually equivalent to the EFZ of the A-P Act. The zone should include all the reasonable inferred fault-rupture hazard of both the main fault and secondary faults, and should account for uncertainties in mapping the fault trace. The guidelines recommend a width of the Warning Zone to be 400 m. Within the Warning Zone, the most detailed level of SM (Level 3 SM) should be mandatory before new construction. Level 3 SM implies a very detailed earthquake geology study of the fault. After completing that study, a new, more accurate fault zoning is achieved. This includes a 30 m-wide Fault Avoidance Zone around the accurately-defined fault trace. If some uncertainties persist after Level 3 studies, such as uncertainties about fault trace location or about the possibility of secondary faulting away from the main fault, the guidelines suggest the use of a wider zone called Susceptible Zone. The guidelines recommend a width of the Susceptible Zone to be 160 m, but the final shape and size of the zone depend on the local geology and the level of accuracy reached during Level 3 SM studies. Both Fault Avoidance and Susceptible Zones can be asymmetric compared with the main fault trace, with recommended footwall to hanging wall ratios of 1:4, 1:2 and 1:1 for normal, thrust and strike-slip faults, respectively.

Nat. Hazards Earth Syst. Sci. Discuss., doi:10.5194/nhess-2017-123, 2017
Manuscript under review for journal Nat. Hazards Earth Syst. Sci.
Discussion started: 19 April 2017

Natural Hazards and Earth System Sciences
Open Access
Discussions

Shape and width of the zones in the Italian guidelines are based mostly on data from normal faulting earthquakes (e.g. Boncio et al., 2012). In general, worldwide the width of the rupture zone (WRZ) for normal and strike-slip earthquakes (e.g. Youngs et al., 2003; Petersen et al., 2011) is much more studied than for thrust earthquakes. Zhou et al. (2010) analysed the width of the surface rupture zones of the 2008 Wenchuan earthquake focusing on the rupture zone close to the main fault, with implications on the setback distance. However, to our knowledge, a global data collection from well-documented surface thrust faulting earthquakes aimed at analysing the characteristics of the WRZ is lacking in the scientific literature.

The objectives of this work are: 1) to collect the data from well-studied surface faulting thrust earthquakes globally (we analysed 10 earthquakes with magnitudes ranging from 5.4 to 7.9); 2) to analyse statistically the distribution of surface ruptures compared to the main fault and the associated WRZ; and 3) to compare the results with the contemporary Italian guidelines and discuss the implications for earthquake fault zoning.

2 Methodology

This work analyses the data from 10 well-studied historic surface faulting thrust earthquakes occurred worldwide during the last few decades (Table 1). These historic earthquakes range in magnitude (Mw) from 5.4 to 7.9 and belong to different tectonic settings, such as continental collision (Spitak, 1988; Kashmir, 2005; Wenchuan, 2008), fold-and-thrust belt (El Asnam, 1980), oceanic-continental collision (Chi-Chi, 1999), transform plate boundary (San Fernando, 1971; Coalinga-Nunez, 1983) and intraplate regions (Marryat Creek, 1986; Tennant Creek, 1988; Killari, 1993).

For the purpose of this work, the following parameters were collected from the literature listed in Table 1: i) displacement (vertical, horizontal and net slip, if available) on the main fault and coordinates of the referred measurement points; ii) distance from the main fault to the secondary ruptures (r in Fig. 1), distinguishing between the ones on hanging wall and on footwall; iii) displacement on secondary faults (if available); iv) width of the rupture zone (WRZ), distinguishing between the ones on hanging wall and on footwall; and v) scarp type (Fig. 2).

When available, the surface rupture data was collected directly from the literature (e.g., Chi-Chi, 1999; Wenchuan, 2008), but in most of the other cases the rupture data was measured from published maps that wereGIS-georeferenced for the purpose of this work. Figure 1 displays the technique used for measuring the distance between the main fault and the secondary ruptures, which allowed us to sample the rupture zone systematically and in reasonable detail. The accuracy of the measurements depends on the scale of the original maps and on the level of detail reported in the maps. In this work only the detailed maps were considered, uncertain or inferred ruptures were not taken into account.

Concerning the scarp type, thrust earthquakes are characterized by a high variability of coseismic scarps due to the complex interaction between faulting and folding, geometry of the faults, and topography and rheology of the surface materials. The coseismic scarps can be classified according to the scheme first proposed by Philip et al. (1992) after the 1988 Spitak (Armenia) earthquake, integrated with the classification of Yu et al. (2010), which includes seven main types of thrust-related fault scarps and related secondary structures (Fig. 2). In case of steeply dipping faults, a simple thrust scarp in bedrock (type a) or a hanging wall collapse scarp in bedrock or in brittle unconsolidated material (type b) are produced. In case of low-angle faults and presence of soft-sediment covers, a number of pressure ridges (types c to f) can be observed, depending on the displacement, sense of slip and behaviour of near-surface materials. In presence of blind faults, a fault-related fold scarp may be formed (type g). Moreover, in this study also two additional types of thrust scarps were distinguished, which are characterized by the occurrence of bending-moment and flexural-slip secondary faults (Yeats, 1986), associated with large-scale folds (hundreds of meters to kilometres in wavelength). Both of them occurred widely during the 1980 El Asnam earthquake (Philip and Meghraoui 1983). Bending-moment faults (type h) are normal faults that are formed close to the hinge zone of large-scale anticlines (extensional faults at the fold extrados in Philip and Meghraoui 1983), while flexural-slip faults (type i) are faults that are formed due to differential slip along bedding planes on the limbs of a bedrock fold (Yeats, 1986). Similar secondary ruptures, associated to small-scale folds (meters to dozens of meters in wavelength), which form at the leading edge of the thrust, are not included in these two particular types.

The measured rupture data has been classified according to the scarp types illustrated in Fig. 2 whenever possible; alternatively, the scarp type was classified as “Unknown”.

3 Width of the Rupture Zone (WRZ): statistical analysis

The most impressive and recurrent measured features are ruptures occurring along pre-existing fault traces and on the hanging wall, as the result of the reactivation of the main thrust at depth. Secondary structures are mainly represented by synthetic and antithetic faults, which are parallel to or branching from the main fault. Fault segmentation and en échelon geometries are common in transfer zones or in oblique-slip earthquakes.

The collected data was analysed in order to evaluate the width of the rupture zone (WRZ), intended as the total width, measured perpendicularly to the main fault, within which all the secondary ruptures occur. Figure 3 shows frequency distribution histograms of the distance of secondary ruptures from the main fault (r) for all the analysed earthquakes. Negative values refer to the footwall, while positive values refer to the hanging wall. In particular, in Fig. 3a we distinguished the scarps with bending-moment (B-M) or flexural-slip (F-S) secondary faults from the other types; in Fig. 3b the scarps without B-M or F-S secondary faults are distinguished by scarp types, and in Fig. 3c the scarps with B-M or F-S secondary faults are distinguished by earthquake. In general, although the values span over a large interval (-750 m to 1,610 m), most of them occur in the proximity of the main fault and display an asymmetric distribution between hanging wall and footwall.

In Fig. 3b all the data (excluding scarps with B-M and F-S faults) are distinguished by scarp type. Simple Pressure Ridges (in green) prevail and the relative data, together with those associated to the other pressure ridges (oblique, back-thrust and low-angle), span over an interval that is larger than for simple thrust scarps (in blue). This implies that the main thrust geometry and the near-surface rheology have a significant control in strain partitioning with consequences on the WRZ.

The occurrence of B-M or F-S secondary faults is strictly related to the structural setting of the earthquake area. In particular, B-M faults, which are related to the presence of large-scale hanging wall anticlines, were clearly observed in the El Asnam 1980 (Philip and Meghraoui, 1983) and Kashmir 2005 (southern part of central segment; Kaneda et al., 2008; Sayab and Khan, 2010) earthquakes. A wide extensional zone (1.8 km-long in the E-W direction; 1.3 km-wide) formed on the eastern hanging wall side of the Sylmar segment of the San Fernando 1971 surface rupture. The interpretation of such an extensional zone is not straightforward. Nevertheless, the presence of a macro-anticline in the hanging wall of the Sylmar fault is indicated by subsurface data (Mission Hill anticline; Tsutsumi and Yeats, 1999). Though it is not possible to clearly classify these structures as B-M faults in strict sense, it seems reasonable to interpret them as generic fold-related secondary extensional faults. Therefore, they were plotted in Fig.s 3a and 3c together with B-M and F-S faults. F-S faults were observed on the upright limb of a footwall syncline in the El Asnam 1980 earthquake. As shown in Fig. 3a, the B-M and F-S datasets contribute significantly in widening the WRZ and are distributed only on the hanging wall or on the footwall of the main fault, respectively. Notably, the distribution of the B-M faults for the El Asnam earthquake is very similar to the distribution of extensional ruptures for the San Fernando earthquake (Fig. 3c). Ruptures close to the main fault ($r < 200$ m) are due to processes operating in all the other types of scarps (Fig. 3b), but for larger distances ($r > \sim 300$ m) they can be related to folding of a large-scale anticline, with a larger frequency between 300 and 1,000 m from the main fault. The B-M ruptures for the Kashmir 2005 earthquake are localized in a narrower zone (≤ 200 m) closer to the main fault, due to the shorter wavelength of the hosting anticline.

In order to analyse the statistical distribution of "r", the collected data was fitted with a number of probability density functions by using the commercial software EasyFitProfessional©V.5.6 (http://www.mathwave.com), which finds the probability distribution that best fits the data and automatically tests the goodness of the fitting. Considering that the width of the rupture zone for the scarps with B-M and F-S is strictly related to the structural setting of the area (presence and wavelength of the fold), in this study only the scarp types without B-M and F-S (called here "simple thrust ruptures") were analysed. The aim is to find a criterion for removing the outliers and sizing the zones within which surface fault ruptures are expected to occur. The hanging wall and footwall data was fitted separately and the results are synthesized in Fig. 4, where the best fitting distribution curves and the cumulative curves, selected by the software according to the Kolmogorov-Smirnov test, are shown. The same continuous function was found for both the hanging wall and footwall, which is the Birnbaum-Saunders (Fatigue Life) distribution.

The hanging wall data (Figs. 4a and 4b) has a modal value of 5.5 m. The 90% probability (0.9 of the cumulative distribution function, HW90) seems to be a reasonable value to cut the outliers (flat part of the curves). It corresponds to a distance of ~320 m from the main fault. The histogram (Fig. 4b) shows a zone close to the main fault, bounded by the 40% probability, where most of the ruptures occur (HW40, corresponding to ~30 m from the main fault). A second sharp drop of the data in the histogram occurs at the 50% probability (HW50, corresponding to ~45 m from the main fault). Also the 3rd quartile is shown (HW75), corresponding to a distance of ~140 m from the main fault. The widths of the zones for the different probabilities (90%, 75%, 50% and 40%) are listed in Table 2.

The footwall data (Figs. 4c and 4d) has a modal value of the best fitting probability density function of 4 m. By applying the same percentiles used for the hanging wall, a 90% cut (FW90) was found at a distance of ~145 m from the main fault. The FW75, FW50 and FW40 correspond to distances of ~70 m, ~25 m and ~20 m from the main fault, respectively (Table 2). It is worth noting that also for the footwall the 40% probability bounds reasonably well the zone where the most of the ruptures occur.

The ratio between the width of the rupture zone on the footwall and the width of the rupture zone on the hanging wall ranges from 1.5 to 2.2 (Table 2), and therefore it is always close to 1:2 independently from the used percentile.

In Fig. 5 the total width of the rupture zone (WRZ tot = WRZ hanging wall + WRZ footwall) is plotted against the displacement on the main fault (vertical component, VD) for the subset of data having displacement information. Though a broad positive correlation between total WRZ and VD can be speculated, especially if the data with B-M and F-S faults is excluded, a clear correlation is not obvious (Fig. 5a). A possible correlation can be found by zooming in the diagram in the area close to the main fault (WRZ <200 m, Fig. 5b). Close to the main fault (WRZ < 60 m), the width of the rupture zone appears to have a nearly linear upper boundary which correlates positively with VD, for VD < ~2 m (dashed line in Fig. 5b). This suggests that close to the main fault the width of the rupture zone increases with displacement, from a minimum of nearly 20 m for decimetric VD up to 50-60 m for VD close to 2 m. However, also for VD <2 m, the maximum WRZ, including the secondary ruptures away from the main fault, can be up to 200 m or wider.

4 Comparison with Italian guidelines and implications for fault zoning during seismic microzonation

The definition of the WRZ based on the analysis of the data from worldwide thrust earthquakes can support the evaluation and mitigation of SFRH. The values reported in Table 2 can be used for shaping and sizing fault zones (e.g. Warning or Susceptible Zones in the Italian guidelines; Earthquake Fault Zones in the A-P Act) and avoidance zones around the trace of active thrust faults.

In Table 3, the total WRZ from the present study is compared with the sizes of the zones proposed by the Italian guidelines for SM studies (Technical Commission for Seismic Microzonation, 2015; SM Working Group, 2015). The table can be considered as a proposal for integrating the existing criteria. The first observation is that the FW:HW ratio proposed by the Italian guidelines is supported by the results of this study (FW:HW ratio close to 1:2).

Assuming that the 90% probability is a reasonable criterion for cutting the outliers from the analysed population, the resulting total WRZ (HW + FW) is 465 m. This width could be used for zoning all the reasonably inferred fault rupture hazard, from both the main fault and secondary faults, during basic (Level 1) SM studies, which do not require high-level specific investigations. The obtained value is not very different from that recommended by the Italian guidelines for Level 1 SM (400 m).

The most evident difference between our proposal and the Italian guidelines concerns the width of the zone that should be avoided, due to the very high likelihood of having surface ruptures. Though the entire rupture zone could be hundreds of meters wide, 40-50% of secondary ruptures are expected to occur within a narrow, 50-70 m wide zone. As could be expected, only site-specific paleosismologic investigations can quantify the hazard from surface faulting at a specific site.In the absence of such a detail, and for larger areas (e.g. municipality scale) the fault avoidance zone should be in the order of 50-70 m, shaped asymmetrically compared to the trace of the main fault (30-45 m on the HW; 20-25 m on the FW). Figure 5b suggests a positive relation between the displacement on the main fault and the width of the rupture zone close to the main fault (WRZ ≤ 60 m). Assuming that this relation is real, Fig. 5b suggests that the avoidance zone should be larger than 20-30 m, even for displacements of a few decimetres.

In Table 3 a width of 210 m is proposed for the susceptible zone (Level 3 SM). The choice of defining the width of the zone as the 3rd quartile (3 out of 4 probability that secondary faulting lies within the zone) is rather arbitrary. In fact, the width of the susceptible zone should be flexible. Susceptible zones are used only if uncertainties remain also after high-level seismic microzonation studies, such as uncertainties on the location of the main fault trace or about the possibility of secondary faulting away from the main fault. Susceptible zones can also be used for areas where a not better quantifiable distributed faulting might occur, such as in structurally complex zones (e.g. stepovers between main fault strands).

It is important to underline that the proposed criteria are applicable only to simple thrust ruptures, without B-M or F-S faults. B-M and F-S secondary faults are strictly related to the structural setting of the area (large-scale folding). Therefore, knowledge of the structural setting of the area may help in identifying zones potentially susceptible to B-M or F-S faulting. In fact, the B-M surface-ruptures commonly observed in historical earthquakes are normal faults. B-M normal faults are expected to occur in the shallowest convex (lengthened) layer of the folded anticline. They can occur only where the bending stress is tensional, that is the convex side of the folded layer, preferentially close to the crest of the anticline and parallel to the anticline hinge. F-S faults can rupture the surface where steeply-dipping limbs of folds associated to the seismogenic thrust, formed by stiff strata able to slip along bedding planes, intersect the topography (e.g. Fig. 2i). Thus, zones of potential B-M or F-S secondary faulting can be traced by knowing the geometry and wavelength of the fold and the first order stiffness of the folded material. Moreover, it is known that coseismic B-M or F-S faults often reactivate pre-existing fault scarps (e.g. Yeats, 1986) being the geomorphic signature which might help in zoning the associated SFRH.

5 Conclusions

The distribution of coseismic surface ruptures (distance of secondary ruptures from the main fault) for 10 well-documented historical surface faulting thrust earthquakes ($5.4 \leq M \leq 7.9$) provide constraints on the general characteristics of the surface rupture zone, with implications for zoning the surface rupture hazard along active thrust faults.

Secondary ruptures can occur up to large distances from the main fault (~750 m on the footwall and ~1,600 m on the hanging wall), but most of them occur within few dozens of meters from the main fault. The distribution of secondary ruptures is asymmetric, with most of them located on the hanging wall. Coseismic folding of large-scale folds (hundreds of meters to kilometres in wavelength) may produce bending-moment (B-M) or flexural-slip (F-S) secondary faults on the hanging wall and footwall, respectively, widening significantly the rupture zone.

The distribution of secondary ruptures for simple thrust ruptures (without B-M and F-S faults) can be fitted by a continuous probability density function, of the same form for both the hanging wall and footwall. This function can be used for removing outliers from the analyzed database (e.g. 90% probability) and define cold criteria for shaping SFRH zones. These zones can be used during seismic microzonation studies.

The 90% probability of the cumulative distribution function defines a rupture zone of ~320 m-wide on the hanging wall and ~145 m-wide on the footwall (total width of ~465 m). This wide zone could be used for zoning SFRH during basic seismic microzonation studies (i.e. Level 1 SM according to the Italian guidelines), which typically lack of specific investigations and therefore are characterized by uncertainties on the location of the main fault and on the occurrence of secondary faulting away from the main fault.

More than 40-50% of the ruptures are expected to occur within a zone of 30-45 m-wide on the hanging wall and 20-25 m-wide on the footwall (total width being 50-70 m). This narrow zone could be used for defining the fault avoiding zone during high-level, municipality-scale seismic microzonation studies (i.e. Level 3 SM according to the Italian guidelines).

A possible positive relation between the displacement on the main fault and the total width of the rupture zone (total WRZ) is found only close to the main fault (total WRZ $\leq$ 60 m). Close to the main fault, the WRZ appears to increase with displacement, from a minimum of nearly 20-30 m for decimetric vertical displacement (VD) up to 50-60 m for VD close to 2 m. This suggests that the avoidance zone should be larger than 20-30 m, even for displacements of a few decimetres.

The average FW:HW ratio of the WRZ is close to 1:2, independently from the used percentile.

In addition to the expected rupture zone along the trace of the main thrust, zones potentially susceptible to B-M or F-S secondary faulting can be inferred by detailed knowledge of the structural setting of the area (geometry, wavelength and lithology of the thrust-related large-scale folds) and by scrutinize possible geomorphic traces of past secondary faulting.

Competing interests

The authors declare that they have no conflict of interest.

Acknowledgements

The project was funded by DiSPUTer, "G. D'Annunzio" University of Chieti-Pescara (research funds to P. Boncio).

References

Avouac, J. P., Ayoub, F., Leprince, S., Konea, O., and Helmberger, V.: The 2006 Mw 7.6 Kashmir earthquake: sub-pixel correlation of ASTER images and seismic waveforms analysis, Earth Planet. Sci. Lett., 249, 514-528, 2006.

Boncio, P., Galli, P., Naso, G., and Pizzi, A.: Zoning Surface Rupture Hazard along Normal Faults: Insight from the 2009 M_W 6.3 L'Aquila, Central Italy, Earthquake and Other Global Earthquakes, Bull. Seism. Soc. Am., 102, 918-935, doi: 10.1785/0120100301, 2012.

Bowman, J. R. and Barlow, B. C.: Surveys of the fault scarp of the 1986 Marryat Creek, South Australia, earthquake, [Australian] Bureau of Mineral Resources, Geology and Geophysics Record 1991/190, 12 pp., 3 plates, 1991.

Bryant, W. A. and Hart, E. W.: Fault-Rupture Hazard Zones in California, Alquist-Priolo Earthquake Fault Zoning Act With Index to Earthquake Fault Zones Maps, Calif Geol. Surv. Spec. Pub., 42, 41 pp, 2007.

Crone, A. J., Machette, M. N., and Bowman, J. R.: Geologic investigations of the 1988 Tennant Creek, Australia, earthquakes— Implications for paleoseismicity in stable continental regions, U.S. Geol. Surv. Bull. 2032-A, A1–A51, 1992.

Fredrich, J., McCaffrey, R., and Denham, D.: Source parameters of seven large Australian earthquakes determined by body waveform inversion, Geoph. J., 95, 1-13, 1988.

Haessler, H., Deschamps, A., Dufumier, H., Fuenzalida, H. and Cisternas, A.: The rupture process of the Armenian earthquake from broad-band teleseismic body wave records, Geophys. J. lnt., 109, 151-161, 1992.

Kaneda, H., Nakata, T., Tsutsumi, H., Kondo, H., Sugito, N., Awata, Y., Akhtar, S. S., Majid, A., Khattak, W., Awan, A. A., Yeats, R. S., Hussain, A., Ashraf, M., Wesnousky, S. G. and Kausar, A. B.: Surface rupture of the 2005 Kashmir, Pakistan, Earthquake and its active tectonic implications, Bull. Seismol. Soc. Am., 98, 521–557, 2008.

Kelson, K. I., Kang, K. H., Page, W. D., Lee, C. T., and Cluff, L. S., 2001: Representative styles of deformation along the Chelungpu Fault from the 1999 Chi-Chi (Taiwan) earthquake: geomorphic characteristic and responses of man-made structures, Bull. Seismol. Soc. Am., 91(5), 930–952, 2001.

Kelson, K. I., Koehler, R. D., Kang, K.-H., Bray, J. D. and Cluff, L. S.: Surface deformation produced by the 1999 Chi-chi (Taiwan) earthquake and interactions with built structures, Final Technical Report, U.S.G.S. Award No. 01-HQ-GR-0122, 21 pp., 2003.

Kerr, J., Nathan, S., Van Dissen, R., Webb, P., Brunsdon, D., and King, A.: Planning for development of land on or close to active faults: A guide to assist resource management planners in New Zealand. Report prepared for the Ministry for the Environment by the Institute of Geological & Nuclear Sciences, Client Report 2002/124, Project Number 440W3301, 2003.

Lettis, W. R., Wells, D. L., and Baldwin, J. N.: Empirical observations regarding reverse earthquakes, blind thrust faults, and quaternary deformation: Are blind thrust faults truly blind?, Bull. Seismol. Soc. Am., 87(5), 1171–1198, 1997.

Lin A., Ouchi T., Chen A., and Maruyama, T.: Co-seismic displacements, folding and shortening structures along the Chelungpu surface rupture zone occurred during the 1999 Chi-Chi (Taiwan) earthquake, Tectonophysics, 330, 225–244, 2001.

Liu-Zeng, J., Sun, J., Wang, P., Hudnut, K. W., Ji, C., Zhang, Z., Xu, Q., and Wen, L.: Surface ruptures on the transverse Xiaoyudong fault: A significant segment boundary breached during the 2008 Wenchuan earthquake, China, Tectonophysics 580, 218–241, 2012.

Liu-Zeng, J., Zhang, Z., Wen, L., Tapponnier, P., Sun, J., Xing, X., Hu, G., Xu, Q., L. Zeng, L., Ding, L., Ji, C., Hudnut, K.W., and van der Woerd, J.: Co-seismic ruptures of the 12 May 2008, Ms 8.0 Wenchuan earthquake, Sichuan: East–west crustal shortening on oblique, parallel thrusts along the eastern edge of Tibet, Earth Plan. Sci. Lett., 286, 355-370, 2009.

Machette, M. N., Crone, A. J., and Bowman, J. R.: Geologic investigations of the 1986 Marryat Creek, Australia, earthquakes - implications for paleoseismicity in stable continental regions, U.S. Geol. Sur. Bull. 2032-B, 29, 1993.

McCaffrey, R.: Teleseismic investigation of the January 22, 1988 Tennant Creek, Australia, earthquakes, Geophys. Res. Lett., 16, 413-416, 1989.

Ota, Y., Watanabe, M., Suzuki, Y., and Sawa, H.: Geomorphological identification of pre-existing active Chelungpu Fault in central Taiwan, especially its relation to the location of the surface rupture by the 1999 Chichi earthquake, Quat. Int., 115–116, 155–166, 2004.

Petersen, M., Dawson, T.E., Chen, R., Cao, T., Wills, C.J.,Schwartz, D.P., and Frankel, A.D.: Fault displacement hazard for strike-slip faults, Bull. Seismol. Soc. Am, 101 (2), 805–825, 2011.

Nat. Hazards Earth Syst. Sci. Discuss., doi:10.5194/nhess-2017-123, 2017
Manuscript under review for journal Nat. Hazards Earth Syst. Sci.
Discussion started: 19 April 2017

Philip, H. and Meghraoui, M.: Structural analysis and interpretation of the surface deformation of the El Asnam earthquake of October 10, 1980, Tectonics, 2, 17-49, 1983.

Philip, H., Rogozhin, E., Cisternas, A., Bousquet, J. C., Borisov, B., and Karakhanian, A.: The Armenian earthquake of 1988 December 7: faulting and folding, neotectonics and palaeoseismicity, Geophys. J. Int., 110, 141-158, 1992.

Rymer, M. J., Kendrick, K. J., Lienkaemper, J. J., and Clark, M. M.: Surface rupture on the Nunez fault during the Coalinga earthquake sequence, in Rymer, M.J, and Ellsworth, W.L. eds., The Coalinga, California, Earthquake of May 2, 1983, U.S. Geol. Sur. Prof. Paper 1487, 299-318, 1990.

Sayab, M. and Khan, M.A.: Temporal evolution of surface rupture deduced from coseismic multi-mode secondary fractures: Insights from the October 8, 2005 (Mw 7.6) Kashmir earthquake, NW Himalaya, Tectonophysics, 493, 58–73, 2010.

Seeber, L., Ekstrom, G., Jain, S.K., Murty, C.V.R., Chandak, N., and Armbruster, J. G.: The 1993 Killari earthquake in central India: a new fault in Mesozoic basalt flows?, J. Geophys. Res., 101, 8543-8560, 1996.

Shin, T.-C. and Teng, T.-L.: An overview of the 1999 Chi-Chi, Taiwan, Earthquake, Article in Bull. Seismol. Soc. Am., 91(5), 895-913, 2001

SM Working Group: Guidelines for Seismic Microzonation, Conference of Regions and Autonomous Provinces of Italy, Civil Protection Department, English edition of: Gruppo di lavoro MS, Indirizzi e criteri per la microzonazione sismica, Conferenza delle Regioni e delle Province autonome – Dipartimento della protezione civile, Roma, 2008, 3 vol. e Dvd, 2015. Available online at http://www.protezionecivile.gov.it/httpdocs/cms/attach_extra/GuidelinesForSeismicMicrozonation.pdf, 2015.

Technical Commission for Seismic Microzonation: Linee guida per la gestione del territorio in aree interessate da Faglie Attive e Capaci (FAC), versione 1.0, Conferenza delle Regioni e delle Province Autonome – Dipartimento della Protezione Civile, 55 pp., Roma, 2015 (In Italian).

Tsutsumi, H. and Yeats, R.: Tectonic setting of the 1971 Sylmar and 1994 Northridge earthquakes in the San Fernando valley, California, Bull. Seism. Soc Am., 89 (5), 1232-1249, 1999.

U.S. Geological Survey Staff: Surface faulting, in: The San Fernando, California, earthquake of February 9, 1971, U.S. Geol. Sur. Prof. Paper 733, 55-76, 1971.

Wells, D. and Coppersmith, K.: New empirical relationships among magnitude, rupture length, rupture width, rupture area, and surface displacement, Bull. Seismol. Soc. Am., 84 (4), 974-1002, 1994.

Nat. Hazards Earth Syst. Sci. Discuss., doi:10.5194/nhess-2017-123, 2017
Manuscript under review for journal Nat. Hazards Earth Syst. Sci.
Discussion started: 19 April 2017

Wesnousky, S. G.: Displacement and geometrical characteristics of earthquake surface ruptures: Issues and implications for seismic hazard analysis and the earthquake rupture process, Bull. Seismol. Soc. Am., 98(4), 1609–1632, 2008.

Xu, X., Wen, X., Yu, G., Chen, G., Klinger, Y., Hubbard, J., and Shaw, J.: Co-seismic reverse- and oblique-slip surface faulting generated by the 2008 Mw 7.9 Wenchuan earthquake, China, Geology 37(6), 515–518, doi 10.1130/G25462A.1., 2009.

Yeats, R. S.: Active Faults Related to Folding, In Active Tectonics: Impact on Society, The National Academies Press, 280 pp. , https://doi.org/10.17226/624, 1986.

Yelding, G., Jackson, J. A., King, G. C. P., Sinvhal H., Vita-Finzi, C., Wood, R. M.: Relations between surface deformation, fault geometry, seismicity, and rupture characteristics during the El Asnam (Algeria) earthquake of the 10 October 1980, Earth Planet. Sci. Lett., 56, 287-304, 1981.

Youngs, Y., W. J. Arabasz, R. R., Anderson, R. E., Ramelli, A. R., Ake, J. P., Slemmons, D. B., McCalpin, J. P., Doser, D. I., Fridrich, C. J., Swan III, F. H., Rogers, A. M., Yount, J. C., Anderson, L. W., Smith, K. D.,Bruhn, R. L., Knuepfer, L. K., Smith, R. B., dePolo, C. M.,.O'Leary, K.W, Coppersmith, K. J., Pezzopane, S. K., Schwartz, D. P., Whitney, J. W., Olig, S. S., and Toro, G. R.: A methodology for probabilistic fault displacement hazard analysis (PFDHA), Earthq. Spectra 19, 191–219, 2003.

Yu, G. H., Xu, X. W., Chen, G. H., Gou, T. T., Tan, X. B., Yang, H., Gao, X., An, Y. F., and Yuan, R. M.: Relationship between the localization of surface ruptures and building damages associated with the Wenchuan 8.0 earthquake, Chinese J. Geophysics, Vol. 52, No. 6, pp. 1294-1311, 2009.

Yu, G., Xu, X., Klinger, Y., Diao, G., Chen, G., Feng, X., Li, C., Zhu, A., Yuan, R., Guo, T., Sun, X., Tan, X., and An, Y.: Fault-Scarp Features and Cascading-Rupture Model for the Mw 7.9 Wenchuan Earthquake, Eastern Tibetan Plateau, China, Bull. Seismol. Soc. Am., Vol. 100, No. 5B, pp. 2590-2614, 2010.

Zhang, Y. S., Shi, J. S., Sun, P., Yang, W., Yao, X., Zhang, C. S., and Xiong T. Y.: Surface ruptures induced by the Wenchuan earthquake: Their influence widths and safety distances for construction sites, Eng. Geol. 166, 245–254, 2013.

Zhou, Q., Xu, X., Yu, G., Chen, X., He, H., and Yin, G.: Width Distribution of the Surface Ruptures Associated with the Wenchuan Earthquake: Implication for the Setback Zone of the Seismogenic Faults in Post-earthquake Reconstruction, Bull. Seismol. Soc. Am., Vol. 100, No. 5B, pp. 2660-2668, 2010.

Nat. Hazards Earth Syst. Sci. Discuss., doi:10.5194/nhess-2017-123, 2017
Manuscript under review for journal Nat. Hazards Earth Syst. Sci.
Discussion started: 19 April 2017

Table 1 Earthquakes used for calculating the width of the rupture zone (WRZ).

Earthquake	Date	Magnitude	Kin. #	SRL*(km)	MD* (m)	Depth (km)	References for earthquake parameters (a) and WRZ calculation (b)
San Fernando, CA, USA	1971.02.09	M_s 6.5, M_w 6.6	R-LL	16	2.5	8.9 (USGS)	a) 1 b) 2
El Asnam, Algeria	1980.10.10	M_s 7.3, M_w7.1	R	31	6.5	10 (USGS)	a) 1 b) 3, 4, 5
Coalinga (Nunez), CA, USA	1983.06.11	M_s5.4, M_w5.4	R	3.3	0.64	2.0 (USGS)	a) 1 b) 6
Marryat Creek, Australia	1986.03.30	M_s5.8, M_w5.8	R-LL	13	1.3	3.0	a) 1, 7 b) 8, 9
Tennant Creek, Australia	1988.01.22 (3 events)	M_s 6.3, M_w 6.3 M_s 6.4, M_w 6.4 M_s 6.7, M_w 6.6	R R-LL R	10.2 6.7 16	1.3 1.17 1.9	2.7 3.0 4.2	a) 1, 10 b) 11
Spitak, Armenia	1988.12.07	M_s 6.8, M_w 6.8	R-RL	25	2.0	5.0-7.0	a) 1, 12 b) 13
Killari, India	1993.09.29	M_s 6.4, M_w 6.1	R	5.5	0.5	2.6	a) 14, 15 b) 15
Chi Chi, Taiwan	1999.09.20	M_w 7.6	R-LL	72	12.7	8.0	a) 16, 17 b) 18, 19, 20, 21
Kashmir, Pakistan	2005.10.08	M_w 7.6[vi]	R	70	7.05 (v)	<15.0	a) 22, 23 b) 23, 24
Wenchuan, China	2008.05.12	M_w 7.9	R-RL	240	6.5 (v) 4.9 (h)	19.0 (USGS)	a) 25 b) 26, 27, 28, 29, 30, 31

Kin. (kinematics): R = reverse, LL = left lateral, RL = right lateral.
* SRL = surface rupture length; MD = maximum displacement (vector sum; v = vertical; h = horizontal).
References: 1 = Wells and Coppersmith, 1994; 2 =U.S. Geological Survey Staff, 1971; 3 =Yelding et al., 1981; 4 =Philip and Meghraoui, 1983; 5 =Meghraouiet al 1988; 6 = Rymer et al. 1990; 7 = Fredrich et al., 1988; 8 = Bowman and Barlow, 1991; 9 = Machette et al., 1993; 10 = McCaffrey, 1989; 11 = Crone et al., 1992; 12 = Haessler et al. 1992; 13 = Philip et al. 1992; 14 = Lettis et al., 1997; 15 = Seeber et al. 1996; 16 = Wesnousky 2008; 17 = Shin and Teng, 2001; 18 = Kelson et al., 2001; 19 = Lin et al., 2001; 20 = Kelson et al., 2003; 21 = Ota et al., 2004; 22 = Avouac et al., 2006; 23 = Kaneda et al., 2008; 24 = Sayab and Khan, 2010; 25 = Xu et al., 2009; 26 = Liu-Zeng et al., 2009; 27 = Liu-Zeng et al., 2012; 28 = Yu et al., 2009; 29 = Yu et al., 2010; 30 = Zhou et al., 2010; 31 = Zhang et al., 2013.

Nat. Hazards Earth Syst. Sci. Discuss., doi:10.5194/nhess-2017-123, 2017
Manuscript under review for journal Nat. Hazards Earth Syst. Sci.
Discussion started: 19 April 2017

Natural Hazards and Earth System Sciences
Open Access
Discussions

Table 2 Width of the rupture zone (WRZ) on the hanging wall (HW) and on footwall (FW) and FW to HW ratio for simple thrust ruptures (cases with bending-moment and flexural-slip faults are not included).

Probability *	WRZ **HW**	WRZ **FW**	**Total** WRZ	**FW:HW**
90%	320 m	145 m	465 m	1:2.2
75%	140 m	70 m	210 m	1:2
50%	45 m	25 m	70 m	1:1.8
40%	30 m	20 m	50 m	1:1.5

* Probabilities refer to the cumulative distribution functions of Fig. 4.

Nat. Hazards Earth Syst. Sci. Discuss., doi:10.5194/nhess-2017-123, 2017
Manuscript under review for journal Nat. Hazards Earth Syst. Sci.
Discussion started: 19 April 2017

Table 3 Comparison between fault zone size from Italian guidelines and the Width of the Rupture Zone (WRZ) from the present study (proposal for updating fault zoning for thrust faults) for simple thrust ruptures (cases with bending-moment and flexural-slip faults are not included).

ZONE *	Seismic Microzonation #	Total WRZ§	FW:HW	Italian guidelines
Warning Zone (*Zona di attenzione, ZA*)	Basic (Level 1)	465 m (90% prob., all the reasonably inferred hazard from MF and SF)	1:2^	400 m FW:HW = 1:2
Avoidance Zone (*Zona di rispetto*, ZR)	High-level (Level 3)	50-70 m (40-50% prob., very high hazard)	1:2 ^	30 m FW:HW = 1:2
Susceptible Zone (*Zona di suscettibilità*, ZS)	High-level (Level 3)	210 m (75% prob., precautionary)	1:2	160 m FW:HW = 1:2

* The original names of zones in the Italian guidelines (in Italian) are in italics.
# Different levels of Seismic Microzonation refer to SM Working Group (2015).
§ MF = main fault; SF = secondary faults.
^ The computed values (1:2.2, 1:1.8 and 1:1.5; Table 2) have been simplified to 1:2.

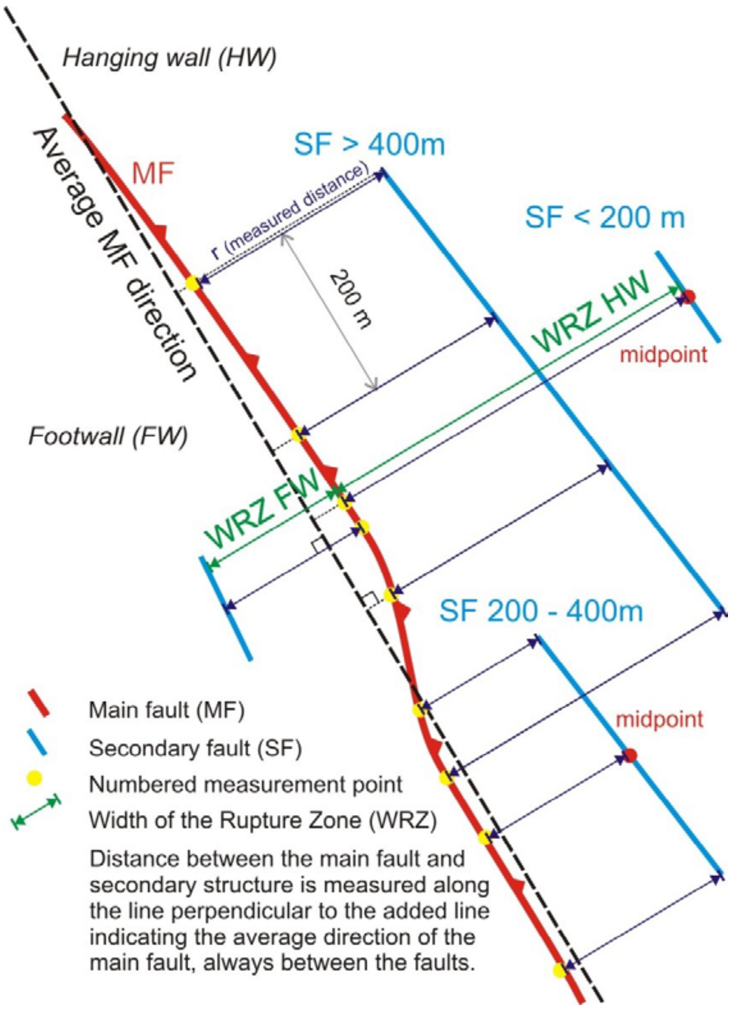

Figure 1: Sketch synthesizing the methodology used for measuring the r and WRZ data.

Natural Hazards and Earth System Sciences
Open Access
Discussions

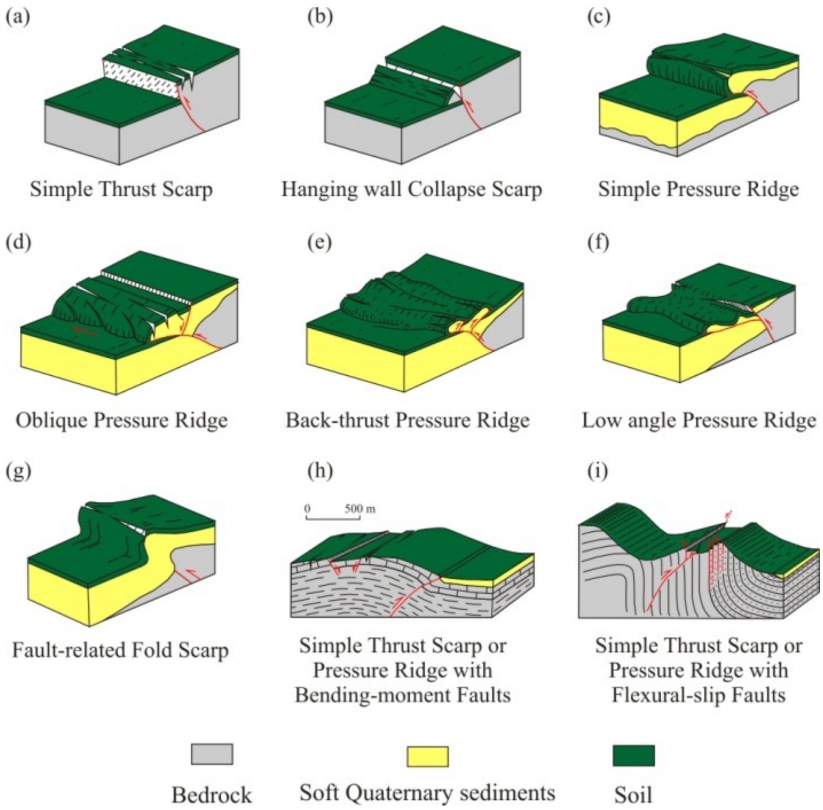

Figure 2: Scarp type classification (modified after Philip et al., 1992 and Yu et al., 2010). The scarp types h) and i) are associated with large-scale folds (hundreds of meters to kilometres in wavelength) and are first reported by Philip and Meghraoui, 1983.

Natural Hazards and Earth System Sciences
Open Access
Discussions

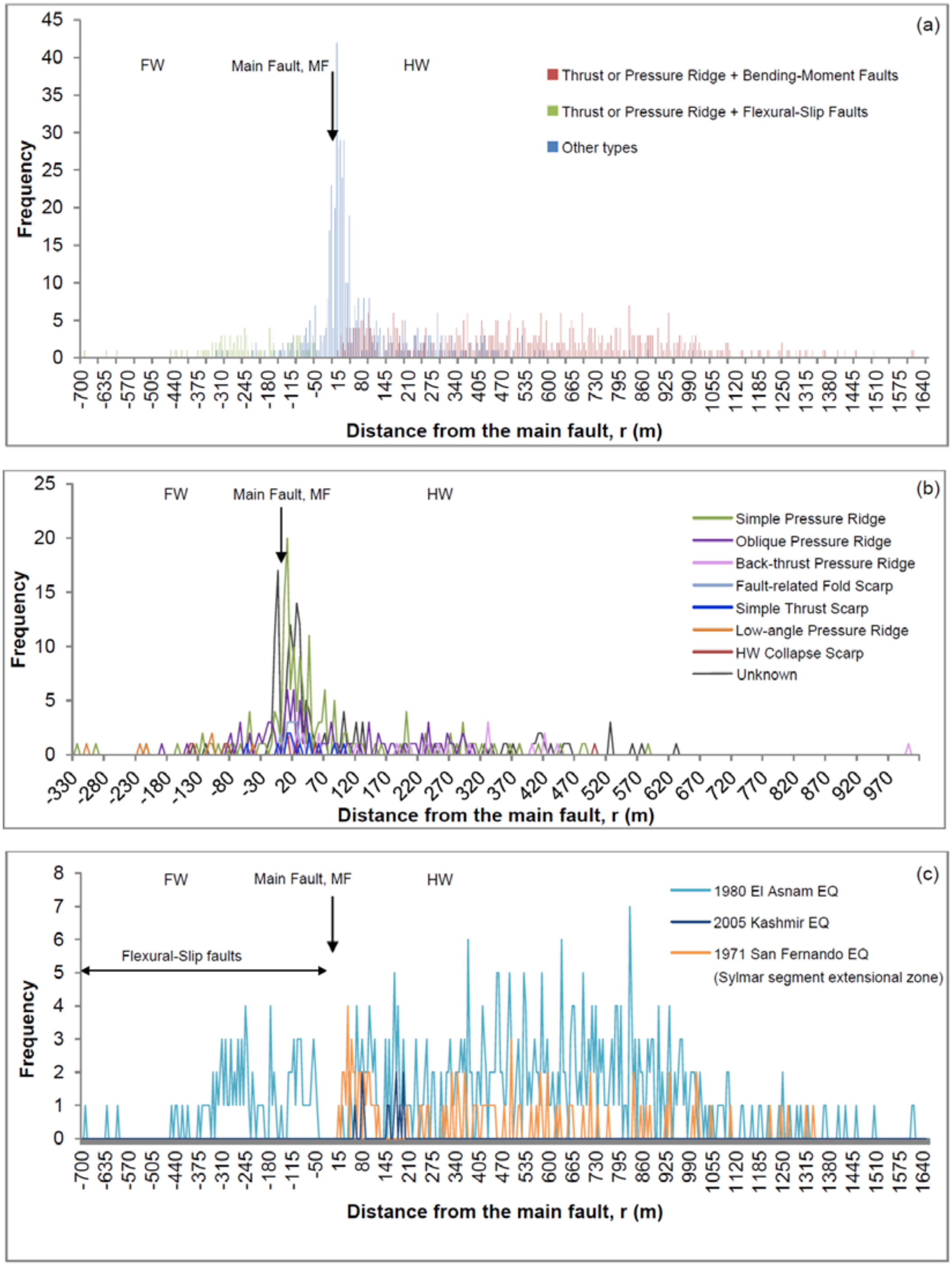

Figure 3: a) Frequency distribution histogram of the rupture distance (r) from the MF for the earthquakes reported in Table 1. The positive and negative values refer to the data on the hanging wall and the footwall, respectively; b) Frequency distribution curves of each scarp type excluding those associated to B-M and F-S faults (types h and i of Fig. 2); c) Frequency distribution curves of the B-M and F-S faults (types h and i of Fig. 2) distinguished by earthquake event.

Nat. Hazards Earth Syst. Sci. Discuss., doi:10.5194/nhess-2017-123, 2017
Manuscript under review for journal Nat. Hazards Earth Syst. Sci.
Discussion started: 19 April 2017

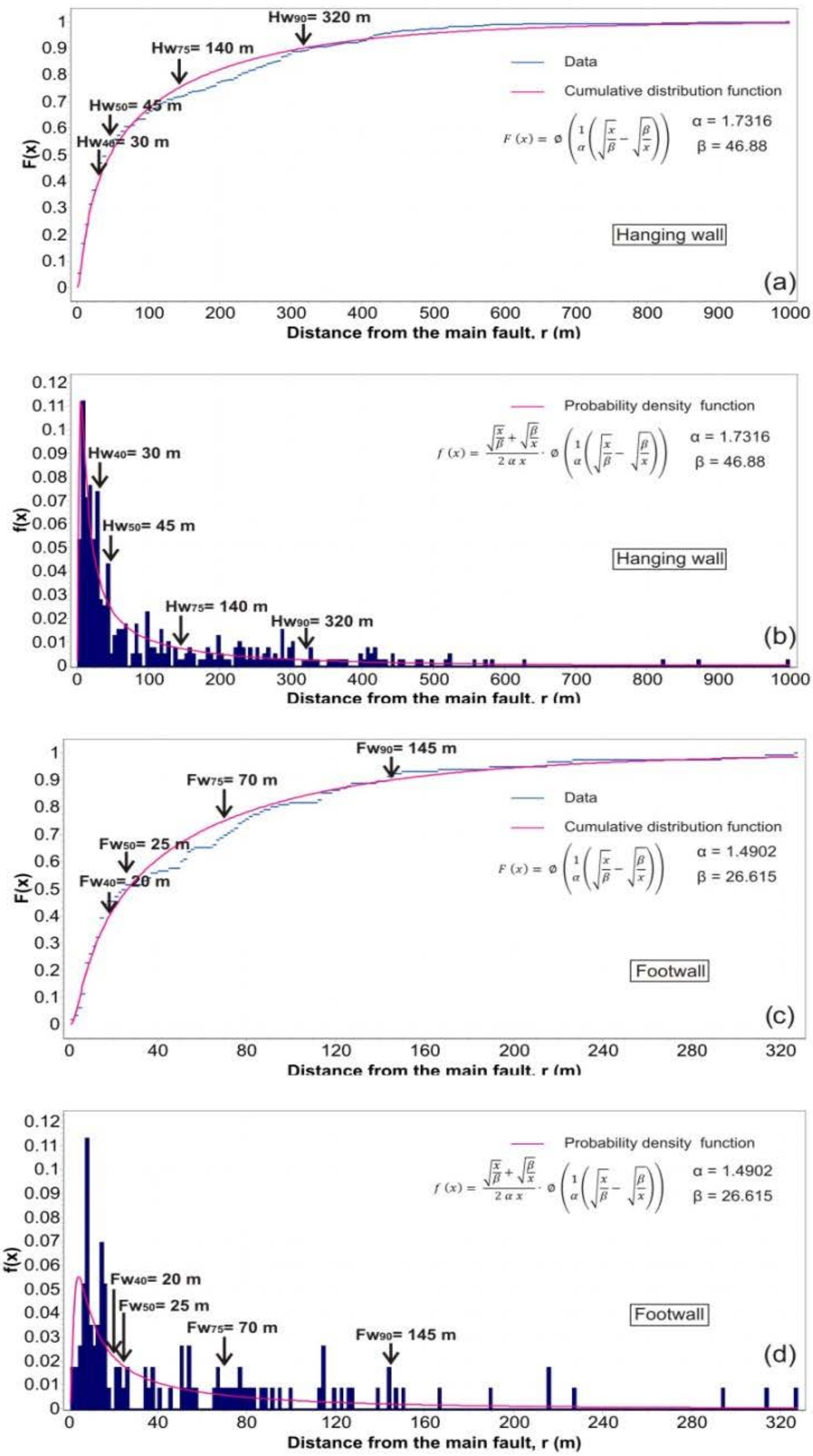

Figure 4: Cumulative distribution function and probability density function of the rupture distance (r) from the MF for the hanging wall (a and b, respectively) and the footwall (b and c, respectively) of the MF. Only the scarp types without associated B-M and F-S faults were analysed.

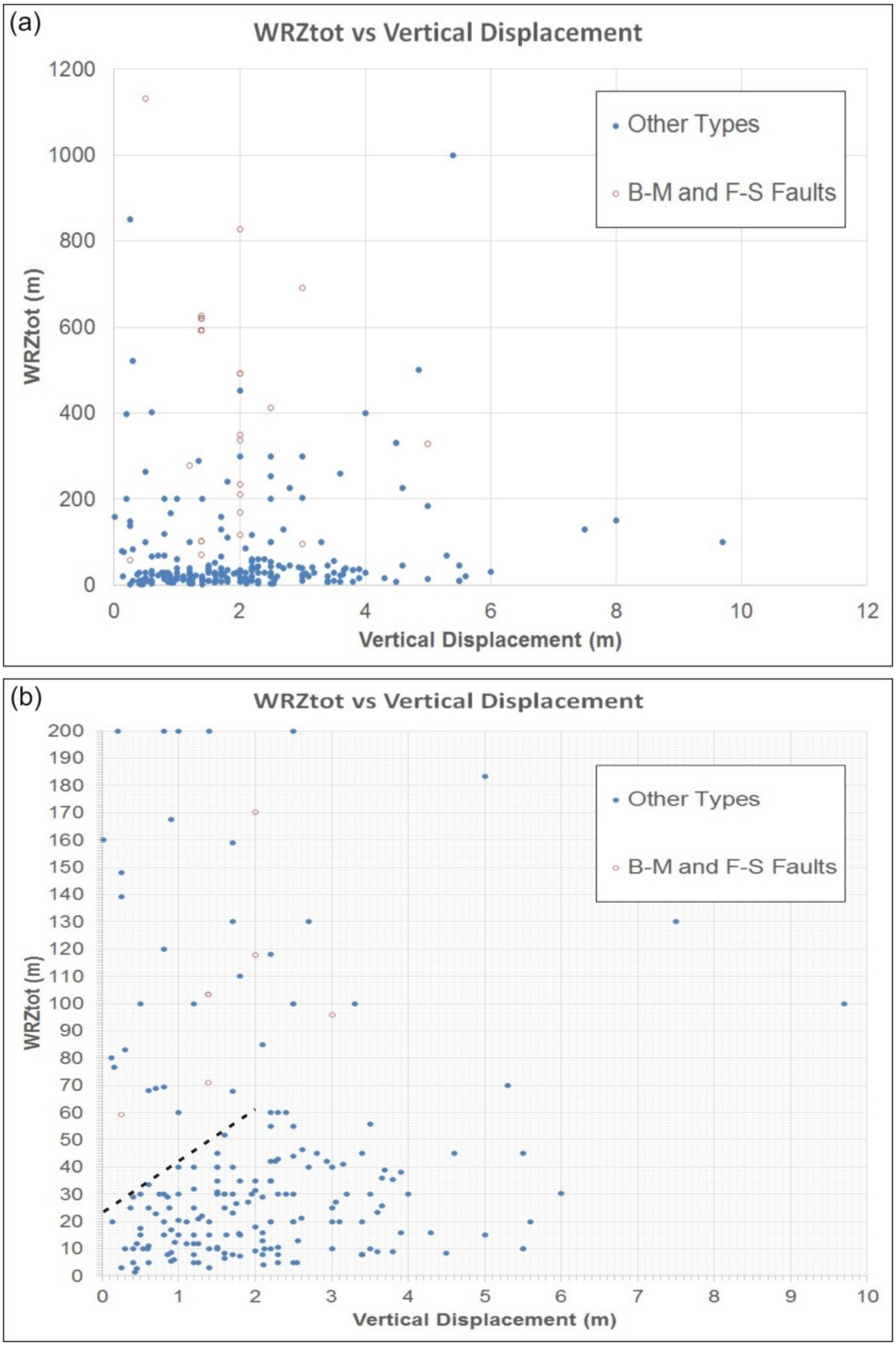

Figure 5 a) Diagram plotting WRZtot (WRZ hanging wall + WRZ footwall) vs. VD (vertical component of the displacement on the MF) for the subset of data having displacement information (see Table 1); b) Enlarged view of the WRZtot vs. VD diagram for WRZtot < 200 m. The dashed line shows the inferred upper bound of the WRZ close to the main fault (WRZ < 60 m).